Early adaptive chromatin remodeling events precede pathologic phenotypes and are reinforced in the failing heart

Douglas J. Chapski[1], Maximilian Cabaj[1], Marco Morselli[4], Rosibel J. Mason[1], Elizabeth Soehalim[1], Shuxun Ren[1], Matteo Pellegrini[4], Yibin Wang[1-3], Thomas M. Vondriska[1-3], Manuel Rosa-Garrido[1*]

Departments of Anesthesiology & Perioperative Medicine[1], Medicine[2], Physiology[3], and Molecular, Cellular & Developmental Biology[4], David Geffen School of Medicine at UCLA

Supplementary data

Supplementary Figure 1. Summary of cardiac physiology measurements. Echocardiographic parameters used to confirm cardiac pathology with CTCFKO (top) or TAC 3 days and TAC 3 weeks (bottom). After 5 weeks tamoxifen diet followed by 1 week regular chow, $Ctcf^{flox/flox}$;αMHCMerCreMer$^{+/-}$ mice show significant increase left ventricular internal dimension in diastole and systole (left and middle, respectively), as well as significant decrease in left ventricular ejection fraction (right) when compared to $Ctcf^{flox/flox}$;αMHCMerCreMer$^{-/-}$ controls. After 3 days TAC, treated mice undergo a slight increase in LVIDd and LVIDs, and a marginal increase in left ventricular ejection fraction, and by 3 weeks TAC we observe a significant increase in left ventricular internal dimension in diastole and systole (left and middle, respectively), and a significant decrease in ejection fraction. Line indicates mean value for the parameter of interest, while the error bars indicate standard deviation (n=10 mice for each condition).

Supplementary Figure 2. Principal components and global analysis of gene expression analyses for RNA-seq and ATAC-seq experiments. (A) Principal component analysis of ATAC-seq data showing separation of 3 days TAC, 3 weeks TAC, and CTCFKO along PC1 (3 biological replicates per condition). Late-stage pathologies (3 weeks TAC and CTCFKO) appear to separate with each other (away from 3 days TAC) along PC1, distinct from control which separates along PC2. **(B)** Principal component analysis of RNA-seq data showing separation of control, 3 days TAC, 3 weeks TAC, and CTCFKO along PC1 (3 biological replicates per condition). CTCFKO is most distinct from the control condition along the first principal component, and the TAC condition separates along PC2 based on early or late stage pressure

overload. **(C)** Venn diagrams indicating the number of significant differentially expressed genes (padj < 0.05) after 3 weeks TAC (left) and 3 days TAC (right); **(D)** CTCFKO (left) and 3 weeks TAC (right); **(E)** CTCFKO (left) and 3 days TAC (right); and **(F)** the three pathologies. Arrows indicate up- and downregulation of mRNA levels. For Venn diagrams in (A-C), pairs of arrows within the intersections refer to the direction of fold change of the comparisons on the left and right sides, respectively.

Supplementary Figure 3. Changes in DNA methylation and chromatin accessibility are consistent between 3 days and 3 weeks TAC, and between TAC and CTCF KO. (A) When comparing CpGs that underwent differential methylation between Control and 3 days TAC, with the CpGs that underwent differential methylation between Control and 3 weeks TAC, 65% of the differentially methylated CpGs were shared between these two comparisons (average methylation difference > 10% and q-value < 0.05; left). In other words, 65% of the differentially methylated regions between control and 3 days were also differentially methylated between control and 3 weeks. Of CpGs that are differentially methylated in both comparisons, the majority (53%) are hypermethylated in both conditions (center). Furthermore, 99.9% of the differentially methylated CpGs shared between the two comparisons (control and 3 days, control and 3 weeks) were found to change in the same direction (right). **(B)** When comparing CpGs that underwent differential methylation between Control and 3 weeks TAC and Control and CTCFKO, 56% of the differentially methylated CpGs were found to be shared (average methylation difference > 10% and q-value < 0.05) with both treatments. Of these, 54% were hypermethylated with both pathologies. 99.8% of the shared

significant CpGs change in the same direction. **(C)** Summary of chromatin accessibility changes analogous to the methylation changes presented in (A). When comparing the ATAC-seq peaks between control and 3 days, with the ATAC-seq peaks between control and 3 weeks, 28% of the differential ATAC-seq peaks in each of these comparisons overlap (left). In other words, 28% of the differentially accessible regions between control and 3 days were also differentially accessible between control and 3 weeks. Of the differential ATAC-seq peaks that were shared between these two comparisons, 62% were found more accessible in both conditions (center). Furthermore, 99% of the differentially accessible peaks shared between the two comparisons (control and 3 days, control and 3 weeks) changed in the same direction (right). **(D)** Chromatin accessibility analysis analogous to the methylation analysis in (B), comparing peaks that are significantly differentially accessible (FDR < 0.05) at 3 weeks TAC and with CTCF depletion. 50% of ATAC-seq consensus peaks are shared between both conditions (left). The overwhelming majority of these change accessibility in the same direction with perturbation (right).

Supplementary Figure 4. Summary of chromatin accessibility and DNA methylation changes with CTCFKO. (A) Gene ontology analysis of genes plus promoters (genes extended by 2000bp) that overlap with the differentially accessible peaks (*left*) and differentially methylated CpGs (*right*) between the control condition and CTCFKO. The *x*-axis indicates -log10(adjusted p-value) for the indicated terms. **(B)** Stacked bar charts indicating significant gene expression change (padj < 0.05) for those genes undergoing significant change in chromatin accessibility (*left*, FDR < 0.05) or in

DNA methylation (*right*, methylation difference > 10% and q-value < 0.05). *Left*, Blue and yellow coloring indicate decrease and increase in chromatin accessibility with CTCFKO, respectively. *Right*, green and purple color indicate hypo- and hypermethylation, respectively. For both stacked bar charts, shading indicates up- (lighter) or downregulation (darker) at the transcript level, respectively.

Supplementary Figure 5. Summary of enhancer methylation and accessibility dynamics. (A) Pie charts showing the percent of enhancers that contain a majority of hypo- (green) or hypermethylated (purple) (average methylation difference > 10% and q-value < 0.05) CpGs with 3 days TAC, 3 weeks TAC, and CTCFKO, in addition to the TAC 3 days → TAC 3 weeks comparison. **(B)** Pie charts showing percent of enhancers that became significantly (FDR < 0.05) more (blue) or less (yellow) accessible between control and 3 days TAC, 3 weeks TAC, and CTCFKO, in addition to the TAC 3 days → TAC 3 weeks comparison.

Supplementary Figure 6. Enhancer methylation plays a role in the transcriptional regulation of subsets of cardiac genes. Analysis accompanying those presented in Figure 2A, indicating percent significantly hyper- (purple) or hypomethylated (green) CpGs after 3 days TAC, in enhancers that interact with differentially expressed (padj < 0.05) genes based on our significant Fit-Hi-C interaction data. Green and red text indicate up- and downregulation of transcript levels, respectively.

Supplementary Figure 7. Binding analysis of epigenetic regulators at enhancers. **(A)** Hypothesized enhancer environments, where enhancers can be hypomethylated and recruit transcriptional activator(s) (*top left*) or inhibitor(s) (*bottom left*) of transcription, or where enhancers can be hypermethylated and prevent recruitment of transcriptional activator(s) (*top right*) or inhibitors (*bottom right*). **(B)** An example locus showing a hypermethylated enhancer (black circles) interacting with the *Rtn4rl1* locus, which undergoes transcriptional activation with 3 weeks TAC. The H3K27ac track (grey) provides evidence supporting existence of the enhancer at the indicated position. Cardiac transcription factor peak positions are shown as blue lines above the signal tracks. **(C)** HOMER motif analysis performed in enhancers with DNA methylation changes (methylation difference > 10% and q-value < 0.05) after inducing heart failure by 3 weeks TAC or depleting CTCF. Motifs resembling several cardiac regulator binding sites (GATA4, TEAD1, NKX2-5, TBX5, p300 and MEF2A) were detected. Motifs in grey were sample-specific. Motif enrichment was calculated with HOMER software, applying a cumulative hypergeometric distribution. **(D)** Summary tables containing p-values from the ChIP-seq peak overrepresentation analyses presented in Figure 2B (*left*) and Figure 5D (*right*). These p-values were calculated as cumulative hypergeometric probabilities.

Supplementary Figure 8. *Cebpd* knockdown abrogates hypertrophic phenotype. (A) RNA-seq track showing transcriptional activation of the C*ebpd* gene at early (TAC 3 days) and late (TAC 3 weeks and CTCFKO) phase disease. **(B)** *Cebpd* RNA levels were significantly reduced 48 hours after siRNA transfection. Relative RNA expression was determined using β-actin as control (n=3 experiments, mean ± S.D.). (C) Cell size measurements showing how *Cebpd* knockdown blocks

hypertrophy of isolated neonatal rat ventricular myocytes in response to phenylephrine (10µM for 48h). n=80 cells from 10 visual fields across 3 independent siRNA transfections. Asterisks indicate significant difference ($p < 0.05$) between indicated groups according to a Wilcoxon rank-sum test.

Loci	Primer name		Sequence
Itga9	Enhancer GATA	(L)	TTGAGGCCAACCTGGTCTAT
		(R)	CTCTGGGACCTCATGCTTGT
	Enhancer H3K27ac	(L)	TGGATTCATGCACATCTGGT
		(R)	AGACAAAATCCGGTGTCTGG
	Promoter GATA	(L)	CCTGTGGCCAAGTCTGTTTT
		(R)	CCAGGATTTATACGGGTTCTTG
	Promoter H3K27ac	(L)	CCTGTGGCCAAGTCTGTTTT
		(R)	CCTTGTGAGGGCTGGAATTA
Nppa	Enhancer Nkx2.5	(L)	GGGCACATGGGGTAAGTTT
		(R)	GAGGTAGAGCCATGGCAGAG
	Enhancer H3K27ac	(L)	GTCAAGCTGGGCAAAGTCTC
		(R)	GGCCAGCACTGTATTCCATT
	Promoter Nkx2.5	(L)	CCTTCCTTCCCCTTGACTTT
		(R)	CCTGAAGCTGGAGGACAGAG
	Promoter H3K27ac	(L)	TGGCCTCCCTCTTTCTACCT
		(R)	GGCTGTCCTGGTCACTTTGT
Mtss1	Enhancer H3K27ac	(L)	ACCGTGCTCTGTGTGTCTTG
		(R)	TCAAATGCCAAATCGAACAA
	Promoter H3K27ac	(L)	TGGGTTTGGATGTGCTGTTA
		(R)	AGGTCTGTGGAGGCAAGAAA

Table 1. Primers used for ChIP-qPCR.

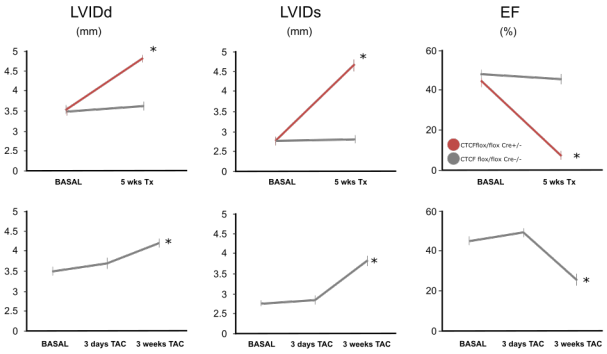

Supplementary Figure 1. Summary of cardiac physiology measurements. Echocardiographic parameters used to confirm cardiac pathology with CTCFKO (top) or TAC 3 days and TAC 3 weeks (bottom). After 5 weeks tamoxifen diet followed by 1 week regular chow, $Ctcf^{flox/flox}$;αMHCMerCreMer$^{+/-}$ mice show significant increase left ventricular internal dimension in diastole and systole (left and middle, respectively), as well as significant decrease in left ventricular ejection fraction (right) when compared to $Ctcf^{flox/flox}$;αMHCMerCreMer$^{-/-}$ controls. After 3 days TAC, treated mice undergo a slight increase in LVIDd and LVIDs, and a marginal increase in left ventricular ejection fraction, and by 3 weeks TAC we observe a significant increase in left ventricular internal dimension in diastole and systole (left and middle, respectively), and a significant decrease in ejection fraction. Line indicates mean value for the parameter of interest, while the error bars indicate standard deviation (n=10 mice for each condition).

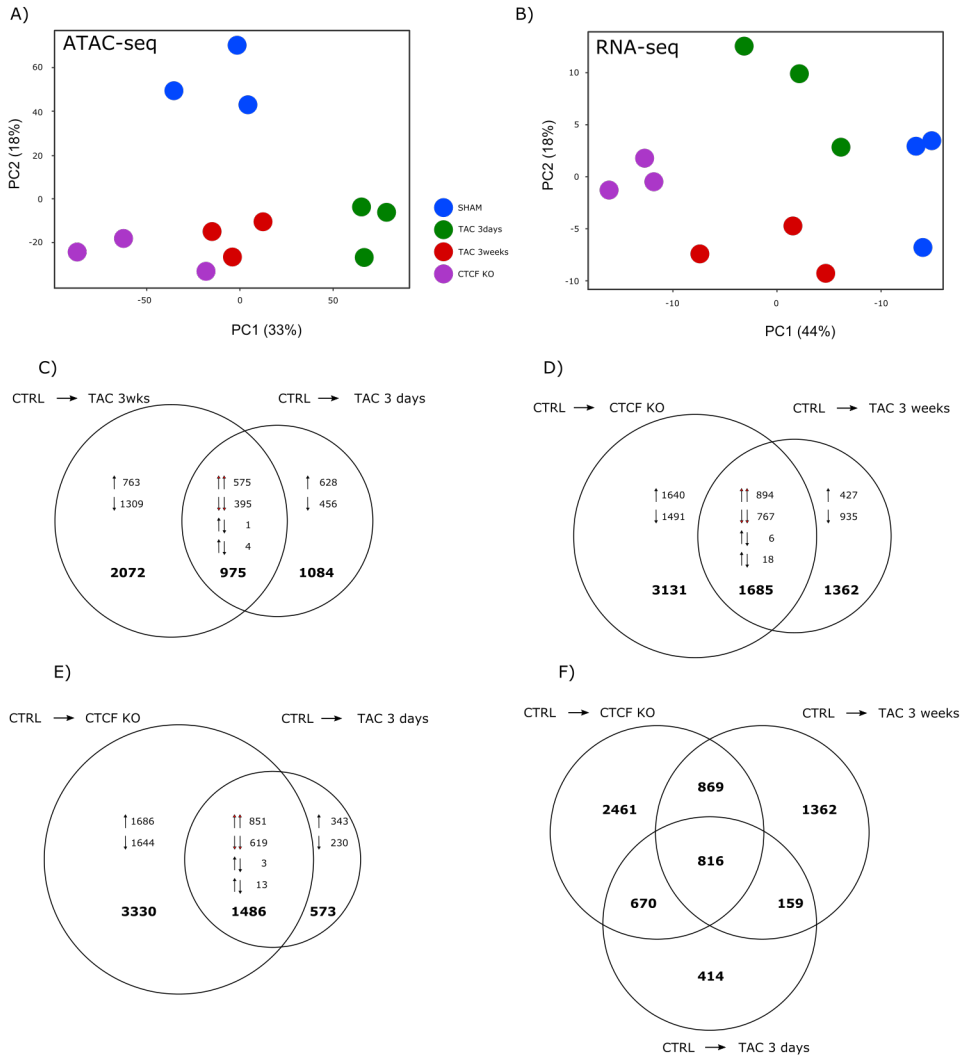

Supplementary Figure 2. Principal components and global analysis of gene expression analyses for RNA-seq and ATAC-seq experiments. (A) Principal component analysis of ATAC-seq data showing separation of 3 days TAC, 3 weeks TAC, and CTCFKO along PC1 (3 biological replicates per condition). Late-stage pathologies (3 weeks TAC and CTCFKO) appear to separate with each other (away from 3 days TAC) along PC1, distinct from control which separates along PC2. **(B)** Principal component analysis of RNA-seq data showing separation of control, 3 days TAC, 3 weeks TAC, and CTCFKO along PC1 (3 biological replicates per condition). CTCFKO is most distinct from the control condition along the first principal component, and the TAC condition separates along PC2 based on early or late stage pressure overload. **(C)** Venn diagrams indicating the number of significant differentially expressed genes (padj < 0.05) after 3 weeks TAC (left) and 3 days TAC (right); **(D)** CTCFKO (left) and 3 weeks TAC (right); **(E)** CTCFKO (left) and 3 days TAC (right); and **(F)** the three pathologies. Arrows indicate up- and downregulation of mRNA levels. For Venn diagrams in (A-C), pairs of arrows within the intersections refer to the direction of fold change of the comparisons on the left and right sides, respectively.

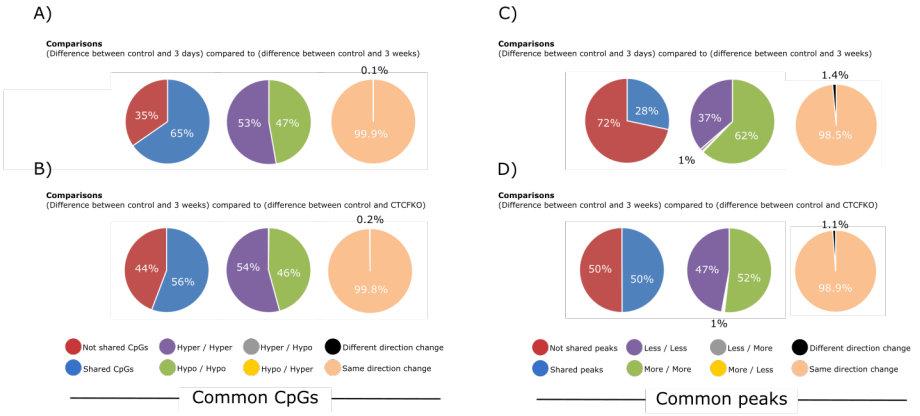

Supplementary Figure 3. Changes in DNA methylation and chromatin accessibility are consistent between 3 days and 3 weeks TAC, and between TAC and CTCF KO. (A) When comparing CpGs that underwent differential methylation between Control and 3 days TAC, with the CpGs that underwent differential methylation between Control and 3 weeks TAC, 65% of the differentially methylated CpGs were shared between these two comparisons (average methylation difference > 10% and q-value < 0.05; left). In other words, 65% of the differentially methylated regions between control and 3 days were also differentially methylated between control and 3 weeks. Of CpGs that are differentially methylated in both comparisons, the majority (53%) are hypermethylated in both conditions (center). Furthermore, 99.9% of the differentially methylated CpGs shared between the two comparisons (control and 3 days, control and 3 weeks) were found to change in the same direction (right). **(B)** When comparing CpGs that underwent differential methylation between Control and 3 weeks TAC and Control and CTCFKO, 56% of the differentially methylated CpGs were found to be shared (average methylation difference > 10% and q-value < 0.05) with both treatments. Of these, 54% were hypermethylated with both pathologies. 99.8% of the shared significant CpGs change in the same direction. **(C)** Summary of chromatin accessibility changes analogous to the methylation changes presented in (A). When comparing the ATAC-seq peaks between control and 3 days, with the ATAC-seq peaks between control and 3 weeks, 28% of the differential ATAC-seq peaks in each of these comparisons overlap (left). In other words, 28% of the differentially accessible regions between control and 3 days were also differentially accessible between control and 3 weeks. Of the differential ATAC-seq peaks that were shared between these two comparisons, 62% were found more accessible in both conditions (center). Furthermore, 99% of the differentially accessible peaks shared between the two comparisons (control and 3 days, control and 3 weeks) changed in the same direction (right). **(D)** Chromatin accessibility analysis analogous to the methylation analysis in (B), comparing peaks that are significantly differentially accessible (FDR < 0.05) at 3 weeks TAC and with CTCF depletion. 50% of ATAC-seq consensus peaks are shared between both conditions (left). The overwhelming majority of these change accessibility in the same direction with perturbation (right).

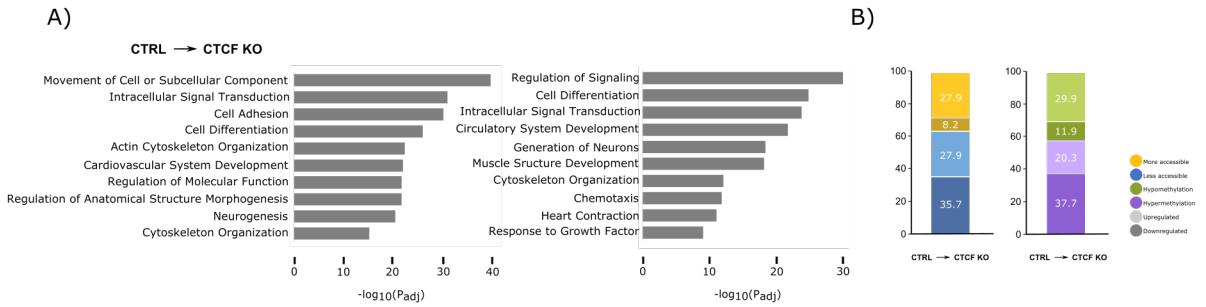

Supplementary Figure 4. Summary of chromatin accessibility and DNA methylation changes with CTCFKO. (A) Gene ontology analysis of genes plus promoters (genes extended by 2000bp) that overlap with the differentially accessible peaks (left) and differentially methylated CpGs (right) between the control condition and CTCFKO. The x-axis indicates -log10(adjusted p-value) for the indicated terms. **(B)** Stacked bar charts indicating significant gene expression change (padj < 0.05) for those genes undergoing significant change in chromatin accessibility (left, FDR < 0.05) or in DNA methylation (right, methylation difference > 10% and q-value < 0.05). Left, Blue and yellow coloring indicate decrease and increase in chromatin accessibility with CTCFKO, respectively. Right, green and purple color indicate hypo- and hypermethylation, respectively. For both stacked bar charts, shading indicates up- (lighter) or downregulation (darker) at the transcript level, respectively.

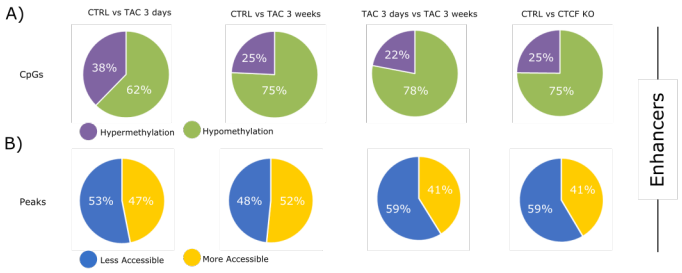

Supplementary Figure 5. Summary of enhancer methylation and accessibility dynamics. (A) Pie charts showing the percent of enhancers that contain a majority of hypo- (green) or hypermethylated (purple) (average methylation difference > 10% and q-value < 0.05) CpGs with 3 days TAC, 3 weeks TAC, and CTCFKO, in addition to the TAC 3 days → TAC 3 weeks comparison. **(B)** Pie charts showing percent of enhancers that became significantly (FDR < 0.05) more (blue) or less (yellow) accessible between control and 3 days TAC, 3 weeks TAC, and CTCFKO, in addition to the TAC 3 days → TAC 3 weeks comparison.

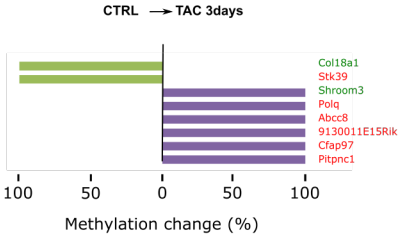

Supplementary Figure 6. Enhancer methylation plays a role in the transcriptional regulation of subsets of cardiac genes. Analysis accompanying those presented in Figure 2A, indicating percent significantly hyper- (purple) or hypomethylated (green) CpGs after 3 days TAC, in enhancers that interact with differentially expressed (padj < 0.05) genes based on our significant Fit-Hi-C interaction data. Green and red text indicate up- and downregulation of transcript levels, respectively.

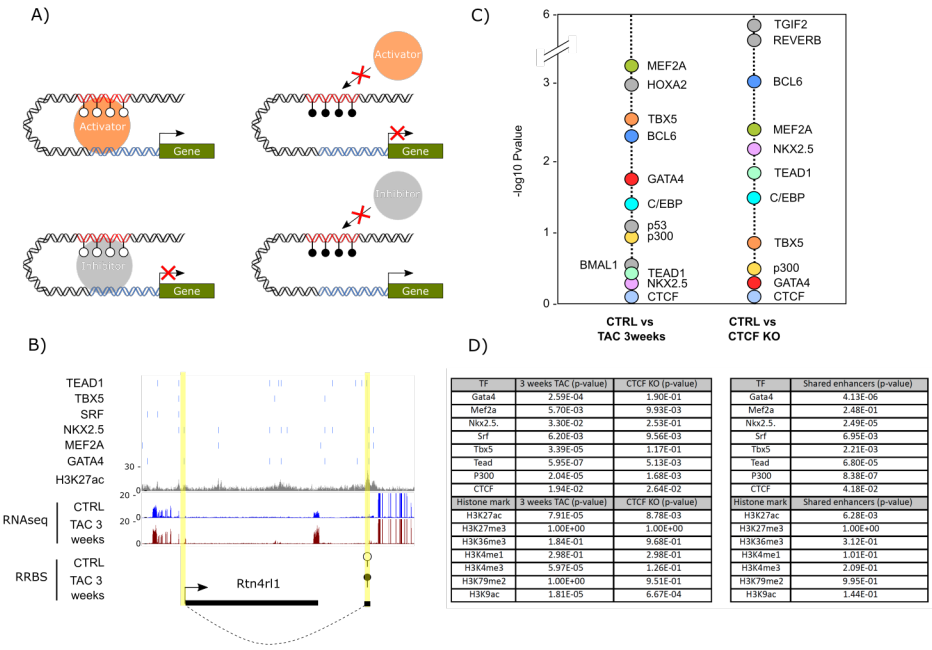

TF	3 weeks TAC (p-value)	CTCF KO (p-value)
Gata4	2.59E-04	1.90E-01
Mef2a	5.70E-03	9.93E-03
Nkx2.5.	3.30E-02	2.53E-01
Srf	6.20E-03	9.56E-03
Tbx5	3.39E-05	1.17E-01
Tead	5.95E-07	5.13E-03
P300	2.04E-05	1.68E-03
CTCF	1.94E-02	2.64E-02
Histone mark	3 weeks TAC (p-value)	CTCF KO (p-value)
H3K27ac	7.91E-05	8.78E-03
H3K27me3	1.00E+00	1.00E+00
H3K36me3	1.84E-01	9.68E-01
H3K4me1	2.98E-01	2.98E-01
H3K4me3	5.97E-05	1.26E-01
H3K79me2	1.00E+00	9.51E-01
H3K9ac	1.81E-05	6.67E-04

TF	Shared enhancers (p-value)
Gata4	4.13E-06
Mef2a	2.48E-01
Nkx2.5.	2.49E-05
Srf	6.95E-03
Tbx5	2.21E-03
Tead	6.80E-05
P300	8.38E-07
CTCF	4.18E-02
Histone mark	Shared enhancers (p-value)
H3K27ac	6.28E-03
H3K27me3	1.00E+00
H3K36me3	3.12E-01
H3K4me1	1.01E-01
H3K4me3	2.09E-01
H3K79me2	9.95E-01
H3K9ac	1.44E-01

Supplementary Figure 7. Binding analysis of epigenetic regulators at enhancers. **(A)** Hypothesized enhancer environments, where enhancers can be hypomethylated and recruit transcriptional activator(s) (top left) or inhibitor(s) (bottom left) of transcription, or where enhancers can be hypermethylated and prevent recruitment of transcriptional activator(s) (top right) or inhibitors (bottom right). **(B)** An example locus showing a hypermethylated enhancer (black circles) interacting with the Rtn4rl1 locus, which undergoes transcriptional activation with 3 weeks TAC. The H3K27ac track (grey) provides evidence supporting existence of the enhancer at the indicated position. Cardiac transcription factor peak positions are shown as blue lines above the signal tracks. **(C)** HOMER motif analysis performed in enhancers with DNA methylation changes (methylation difference > 10% and q-value < 0.05) after inducing heart failure by 3 weeks TAC or depleting CTCF. Motifs resembling several cardiac regulator binding sites (GATA4, TEAD1, NKX2-5, TBX5, p300 and MEF2A) were detected. Motifs in grey were sample-specific. Motif enrichment was calculated with HOMER software, applying a cumulative hypergeometric distribution. **(D)** Summary tables containing p-values from the ChIP-seq peak overrepresentation analyses presented in Figure 2B (left) and Figure 5D (right). These p-values were calculated as cumulative hypergeometric probabilities.

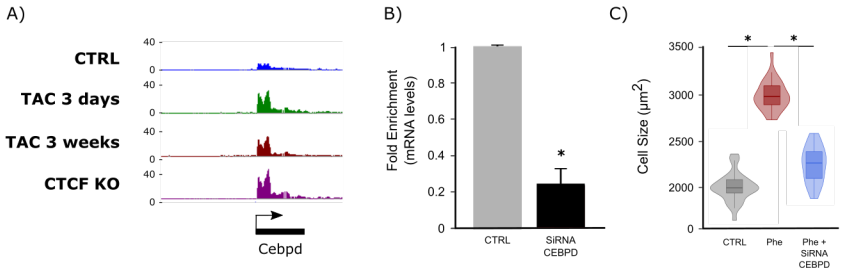

Supplementary Figure 8. *Cebpd* knockdown abrogates hyperthrophic phenotype. (A) RNA-seq track showing transcriptional activation of the Cebpd gene at early (TAC 3 days) and late (TAC 3 weeks and CTCFKO) phase disease **(B)** Cebpd RNA levels were significantly reduced 48 hours after siRNA transfection. Relative RNA expression was determined using β-actin as control (n=3 experiments, mean ± S.D.). **(C)** Cell size measurements showing how Cebpd knockdown blocks hypertrophy of isolated neonatal rat ventricular myocytes in response to phenylephrine (10μM for 48h). n=80 cells from 10 visual fields across 3 independent siRNA transfections. Asterisks indicate significant difference ($p < 0.05$) between indicated groups according to a Wilcoxon rank-sum test.